Science and Technology Indonesia
e-ISSN:2580-4391 *p*-ISSN:2580-4405
Vol. 10, No. 2, April 2025

Research Paper

Nanoparticle-Enhanced 3D-Connector Microfluidic Paper-Based Analytical Device (3D-μPADs) for Sensitive and Cost-Effective Detection of Albumin-Creatinine Ratio in Urine Sample

Akhmad Sabarudin[1*], Saidun Fiddaroini[1], Ahmad Luthfi Fahmi[1], Abdul Munir Roja'i[1], Isadora Evani Salsabila[1], Aulanni'am[1], Arie Srihardyastutie[1], Hani Susianti[2], Nur Samsu[3]

[1]*Chemistry Department, Faculty of Science, Brawijaya University, Malang, 65145, Indonesia*
[2]*Department of Clinical Pathology, Brawijaya University, Dr. Saiful Anwar General Hospital, Malang, 65111, Indonesia*
[3]*Department of Internal Medicine, Faculty of Medicine, Brawijaya University, Malang, 65145, Indonesia*
***Corresponding author**: sabarjpn@ub.ac.id

Abstract
Chronic kidney disease (CKD) is a global health challenge affecting over 800 million people worldwide. Early detection is crucial to prevent progression to end-stage renal disease (ESRD), where life-saving interventions like dialysis or transplantation are necessary. Among the markers for early kidney damage, the Albumin Creatinine Ratio (ACR) in urine is one of the most reliable. Conventional methods of ACR detection, such as LC/MS-MS and ELISA, are highly accurate but require expensive equipment and skilled personnel, limiting their accessibility, especially in resource-limited settings. To address this, we developed a 3D-connector microfluidic paper-based analytical device (3D-μPADs) enhanced with gold nanoparticles (AuNPs) for sensitive and low-cost ACR detection. The integration of AuNPs amplifies colorimetric signals, enhancing the visual distinction in albumin detection. Our 3D-μPADs were fabricated using chromatographic paper Whatman No. 1 with hydrophobic barriers created by solid wax printing, followed by reagent immobilization for albumin and creatinine detection. The colorimetric and distance responses, based on reactions with Bromocresol Green (BCG) and Chrome Azurol S-Palladium (CAS-Pd^{2+}), were analyzed using ImageJ software to quantify albumin and creatinine levels. The 3D-μPADs exhibited optimal sensitivity and accuracy, with linear detection ranges for albumin and creatinine of 30–400 mg/g. Validation with human urine samples demonstrated an accuracy of 93.04%, suggesting that 3D-µPADs offer a promising alternative for early nephropathy detection. Our findings provide a cost-effective, accessible tool for CKD screening, potentially transforming diagnostics in low-resource environments.

Keywords
Albumin, Creatinine, Gold Nanoparticle, Paper-Based Devices, Urine

Received: 15 November 2024, Accepted: 15 February 2025
https://doi.org/10.26554/sti.2025.10.2.504-518

1. INTRODUCTION

The kidneys, though small in size, serve as essential organs for maintaining homeostasis within the human body by performing complex functions of filtration, secretion, and reabsorption (Thompson and Joy, 2022). Their primary responsibility involves the removal of metabolic waste products and excess fluids from the bloodstream, ensuring that harmful compounds are effectively excreted, while simultaneously regulating the body's fluid balance and electrolyte stability (Ariyanti et al., 2018; Park et al., 2018). Beyond waste elimination, the kidneys play a pivotal role in maintaining blood pressure, synthesizing hormones for erythropoiesis, and contributing to bone mineral metabolism (Yang et al., 2014). Impairments in kidney function, broadly referred to as nephropathy, disrupt these processes, leading to an inability to regulate fluid and electrolyte homeostasis effectively, and if left unchecked, can evolve into chronic kidney disease (CKD) (Fraser and Blakeman, 2016).

CKD is characterized by a gradual, often irreversible loss of renal function, which severely affects the body's ability to excrete waste products, resulting in uremia, fluid overload, and a host of metabolic complications (Kovesdy, 2022). This disease represents a significant global health burden, with more than 800 million individuals affected worldwide, translating to over 10% of the population. Alarmingly, CKD-related mortality has escalated by nearly 40% over the past two decades, making it one of the fastest-growing causes of death (Sulehri and Sheikh, 2009). In its advanced stages, CKD leads to end-stage

renal disease (ESRD), where life-saving interventions such as dialysis or kidney transplantation become necessary (Yumang et al., 2021). Thus, the early detection and management of kidney disease are critical to preventing disease progression and reducing mortality.

Among the clinical markers used to assess kidney function, the albumin-creatinine ratio (ACR) in urine stands out as a reliable early indicator of kidney damage. The ratio measures the levels of albumin, a protein that leaks into the urine when kidney function declines, and creatinine, a waste product of muscle metabolism, which serves as a baseline for normalization (Fortova et al., 2018). Elevated ACR values have been closely correlated with increased risks of CKD and cardiovascular disease, making it an invaluable tool in clinical diagnostics. Current techniques to measure ACR include highly sensitive methods such as Flow Injection Analysis (FIA), Liquid Chromatography Tandem Mass Spectrometry (LC/MS-MS) (Sabarudin, 2018), High-Performance Liquid Chromatography (HPLC) (Tkáčiková et al., 2020), and immunoassays such as ELISA (Kiconco et al., 2019). However, these methods, while accurate, are associated with significant limitations in terms of cost, instrument complexity, and the need for skilled operators, which restrict their use, particularly in resource-limited settings (Chapman et al., 2019).

To address the limitations of conventional ACR detection methods, significant advancements have been made in the development of point-of-care diagnostics. One such innovation is microfluidic paper-based analytical device (μPADs), which has garnered attention due to its simplicity, low cost, and adaptability for various diagnostic applications (Sununta et al., 2018). μPADs are typically constructed using cellulose-based materials like Whatman No. 1 paper, combined with hydrophobic barriers to guide fluid flow within microchannels (Cheng et al., 2023). Various fabrication techniques have been employed to create these barriers, including screen printing, photolithography, wax printing, and inkjet printing, enabling μPADs to operate without the need for external pumps or sophisticated instrumentation (Bruzewicz et al., 2008; Carrilho et al., 2009; De Tarso Garcia et al., 2014; Ng and Hashimoto, 2020; Songjaroen et al., 2011; Wang et al., 2012; Yamada et al., 2015).

μPADs have emerged as promising tools for a wide range of biochemical analyses, from glucose monitoring and pathogen detection (Chen et al., 2022; Trinh et al., 2022). To the quantification of heavy metals (Petersson and Philippou, 2016). In the context of kidney disease, μPADs provide a novel platform for ACR measurement, leveraging colorimetric detection methods that allow for the visualization and quantification of protein levels directly on the device (Morbioli et al., 2017). The devices are designed to facilitate rapid, on-site testing, with their capillary action-driven flow providing a means for fluid transport and reaction within defined zones. A common issue with conventional μPADs and distance-based μPADs is uncontrolled capillary fluid flow, which causes reagents to spread from the detection zone to the sample zone, resulting in baseline irreproducibility. To address this problem, the 3D-connector μPADs (3D-μPADs) was developed, which not only allow for better control of capillary flow but also help mitigate interferences by functioning the connector as a masking or separation medium. Furthermore, the development of three-dimensional (3D) connector designs has improved both the resolution and sensitivity of these devices, allowing for more accurate detection of biomarker concentrations while preventing sample contamination (Al-Jaf and Omer, 2022).

The incorporation of gold nanoparticles (AuNP) in microfluidic paper-based analytical devices (μPADs) has led to significant advancements in the detection of albumin-creatinine ratios (ACR) due to the unique properties exhibited by AuNPs (Hardiyanti et al., 2024). Gold nanoparticles possess the ability to amplify detection signals through pronounced color changes, which are pivotal in colorimetric detection systems within μPADs (Kusuma et al., 2023; Yang et al., 2022; Zhang et al., 2020). This phenomenon arises from the specific interactions between AuNPs and albumin, resulting in protein aggregate formation. These interactions yield sharper and more visually discernible color transitions, enabling heightened detection sensitivity even at low albumin concentrations (Dai et al., 2023; Khachornsakkul et al., 2023; Wang et al., 2019).

Albumin is a globular protein composed of 585 amino acid residues and has a molecular weight of approximately 66.5 kDa. It is synthesized at a rate of 9-12 grams per day and its production is regulated by the hormone insulin (Chen et al., 2016). Serum albumin plays a crucial role in maintaining oncotic pressure in blood plasma and acts as a carrier for a variety of endogenous and exogenous compounds, including drugs. Elevated levels of serum albumin can be indicative of several health conditions, including cardiovascular disease, diabetes, and chronic kidney disease (CKD) (Mohamed et al., 2021). Gold nanoparticles offer several advantages, including ease of surface modification, simple synthesis, low toxicity, and potential applications in biosensing, drug delivery, and bioimaging (Bolaños et al., 2019; Harish et al., 2022; Mousavi et al., 2018; Paramasivam et al., 2017). Specifically, in the context of detecting albumin and creatinine, AuNPs are utilized in their colloidal form, which involves dispersing gold nanoparticles in a water solvent (Ajdari et al., 2017).

Creatinine is the end product of creatine metabolism, which occurs in the liver and kidneys from amino acids. In patients with kidney disease, creatinine can accumulate along with non-protein nitrogen (NPN) elements (Srivastava et al., 2009). Creatinine levels are used to assess renal excretory function, especially in chronic kidney disease (CKD). A plasma creatinine concentration of less than 900 μmol/L typically indicates normal glomerular filtration (Decreased, 2013). Compared to plasma urea measurements, creatinine levels provide a more accurate assessment of kidney function. Elevated creatinine levels in urine are indicative of impaired kidney function and can signal the presence of CKD (Randviir and Banks, 2013).

In this work, AuNPs are combined with Bromocresol Green (BCG) reagents to facilitate more contrasting color changes for detection of albumin, thereby enhancing the analysability

of the resulting color response. Furthermore, AuNPs provide excellent stability and compatibility within paper-based microfluidic systems due to their minuscule size and ability to be uniformly dispersed within the reaction zones. For creatinine detection, the Jaffe reaction is commonly used, involving alkaline picrate reagents that cause a color change from yellow to orange (Chaiyo et al., 2018). Another method is ligand-exchange, where the Chrome Azurol S-Palladium (CAS-Pd^{2+}) complex shifts from blue to yellowish when CAS is displaced by creatinine (Hiraoka et al., 2020). This latter method produces a color change that is more visually noticeable. By integrating the advantages of 3D-μPADs with BCG-AuNPs and CAS-Pd^{2+}, our proposed approach offers a promising diagnostic platform, particularly suited for ACR detection in resource-limited settings. The role of BCG-AuNPs and CAS-Pd^{2+} in this 3D-μPADs not only enhances detection accuracy and sensitivity but also enables testing without the necessity for sophisticated laboratory equipment. Consequently, the application of these two reagents for detecting ACR in 3D-μPADs presents an accessible and cost-effective solution for the early screening of chronic kidney disease (CKD), ultimately contributing to a reduction in the global burden of kidney diseases and improving patient care quality worldwide.

2. EXPERIMENTAL SECTION

2.1 Materials

The chemicals used in this study included bovine serum albumin (BSA), sodium hydroxide (NaOH, EMSURE), sodium phosphate heptahydrate ($Na_2HPO_4{\cdot}7H_2O$), sodium dihydrogen phosphate dihydrate ($Na_2HPO_4{\cdot}7H_2O$), ethanol, Chrome Azurol S (CAS), Palladium Chloride ($PdCl_2$), hydrochloric acid (HCl), and Bromocresol Green (BCG), all sourced from Sigma Aldrich (Singapore). Colloidal gold nanoparticles (AuNPs 100 nm, 1.25×10^8 particles/mL) were provided by MaxLab Indonesia. Artificial urine samples were prepared using materials from SIGMA-ALDRICH (Singapore), including citric acid (≤99%), sodium bicarbonate (99.5-100.5%), uric acid (≤99.0%), sodium chloride (≤99.0%), sodium sulfate (≤99.0%), potassium dihydrogen phosphate (≤99.0%), dicalcium hydrogen phosphate (≤99.0%), ammonium chloride (≤99.5%), magnesium sulfate (≤99.0%), and urea.

The study use ImageJ software for color change distance analysis. Whatman No. 1 chromatography paper from GE Healthcare Life Sciences (United Kingdom) was used for fabricating the 3D-μPADs, with hydrophobic barriers printed using solid wax ink (Xerox, USA). CorelDraw Graphics Suite X7 software and a ColorQube 8580DN wax printer (Xerox, USA) were employed to design and print patterns on the Whatman paper.

2.1.1 Paper Device Fabrication

3D-connector microfluidic paper-based analytical devices (3D-μPADs) were designed using CorelDraw Graphics Suite X7 software and printed on Whatman No.1 chromatography paper with a Xerox ColorQube 8580DN solid ink printer. After printing, the design was heat-treated in an oven at 120°C for 3 minutes to ensure proper penetration of the wax. The paper was then trimmed to the desired shape using a paper trimmer, and the back of the 3D-μPADs was coated with tape to prevent leakage and ensure structural integrity. The steps involved in the fabrication and design of the 3D-μPADs are illustrated in Figure 1.

2.1.2 Detection and Analysis of Albumin-Creatinine Based on the Color Change Distance

Albumin detection was performed using Bromocresol Green (BCG) modified with AuNPs. BCG (5mM) was mixed with AuNPs at the volume ratio of 5:1. Then, BCG-AuNPs mixture was applied to the reaction zone on the 3D-μPADs, and then albumin solution was introduced into the sample zone of the 3D-μPADs. This procedure resulted in a color change in the reaction zone, with BCG reacting with the albumin standard solution and transitioning from greenish to bluish. The color change was documented using photographs and analyzed with ImageJ software. This analysis aims to clearly define the reaction length boundary based on the intensity of the generated color (RGB spectra). Different albumin concentrations produced varying distances of color change; higher concentrations led to longer reaction distances.

Palladium chloride ($PdCl_2$) was applied to the reaction zone of the 3D-μPADs, followed by the addition of Chrome Azurol S (CAS). After allowing the 3D-μPADs to dry for 3 minutes, a color change from brown to blue was observed. Subsequently, a creatinine solution was added to the sample zone. This resulted in a color change from blue to yellowish, indicating a ligand exchange reaction involving CAS-Pd^{2+}. The extent of the color change, measured as the reaction distance, correlates with the creatinine concentration; higher creatinine levels result in a longer reaction distance.

Table 1. The Composition of Artificial Urine Solution

Components	Concentration (mM)
Citric acid	2
Urea	170
Uric acid	0.4
Lactic acid	1.1
Potassium dihydrogen phosphate	7
Dipotassium hydrogen phosphate	7
Sodium chloride	90
Sodium sulfate	10
Sodium bicarbonate	25
Ammonium chloride	25
Calcium chloride	2.5
Magnesium sulfate	2

Prior to apply the proposed method to real human urine samples, the 3D-μPADs was examined through measurement of artificial urine containing the mixture of albumin with creatinine at appropriate ratios. The artificial urine is made by

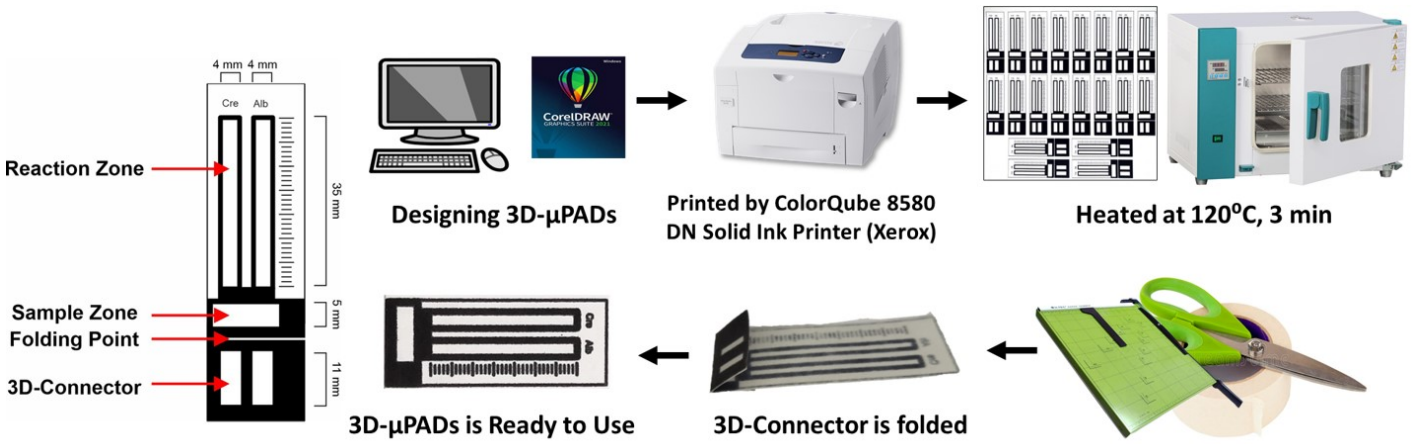

Figure 1. Design and Fabrication Scheme of 3D-μPADs

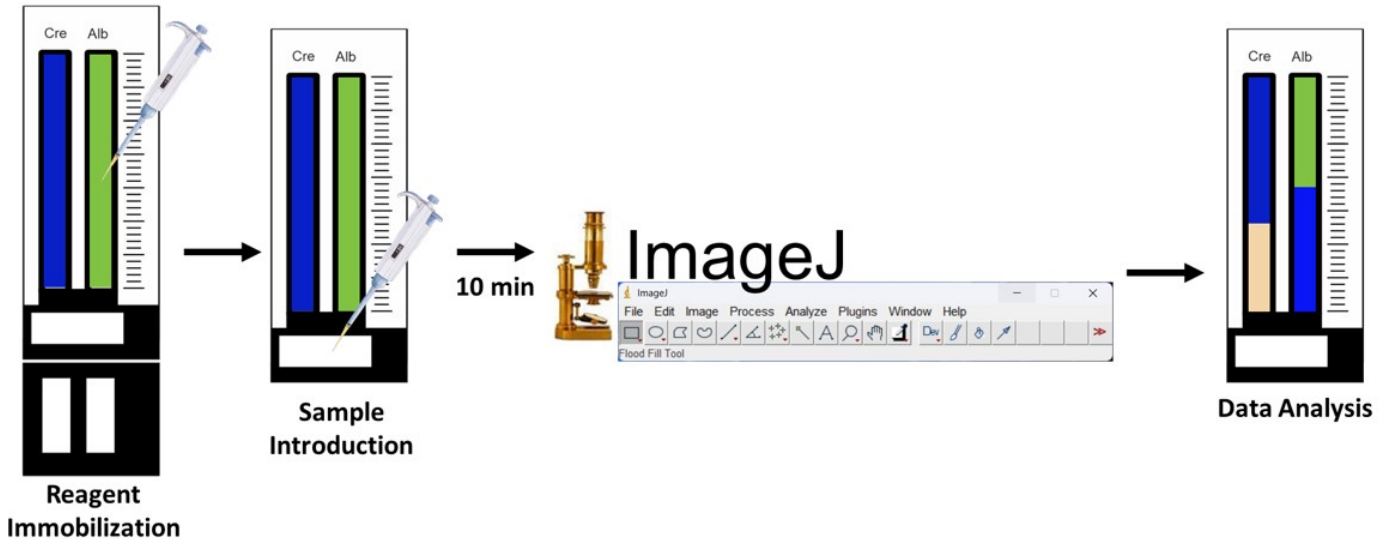

Figure 2. Data Analysis Scheme

mixing some compound as detailed in Table 1. This artificial urine has been adjusted to match the composition of healthy human urine, as reported in other studies (Hiraoka et al., 2020; Sarigul et al., 2019). For this purpose, the CAS-Pd^{2+} reagent was immobilized to the left reaction zone (for creatinine detection, see Figure 1), while the BCG-AuNPs reagent was applied to the right reaction zone (for albumin detection, see Figure 1). After reagents immobilization, the sample was added, and the resulting color changes were analyzed using ImageJ to determine the reaction distances as illustrated in Figure 2.

The analysis using ImageJ to determine the slope intensity can be performed by following the procedure outlined in Figure 3. The observation image is uploaded into the software through the "File" menu on the toolbar, then selecting "Open". Select the “Straight” tool to measure the observed color intensity in the reaction zone. Before starting the analysis, the intensity measurement scale needs to be set by opening the "Analyze" menu, selecting "Set Scale," and adjusting the parameters: "Known distance = 35," "Unit of length = mm," and checking the "Global" option to standardize the measurement scale used. Next, select “Plugin” toolbar, then “Graphics”, and choose “RGB Profile Plot” to analyze the color intensity. Then, click the "List" option to obtain raw color intensity data from the "Plot Values" section. The red color from the RGB intensity is selected due to its good contrast with the observed reaction results. The color intensity data can be transferred to Ms. Excel to determine the highest peak coordinates (x2, y2) and the lowest point coordinates (x1, y1). The slope value of red color intensity can then be calculated according to Figure 3.

2.1.3 Method Validation

The proposed method was validated to assess its linearity, accuracy, and precision. Before validated, the proposed method

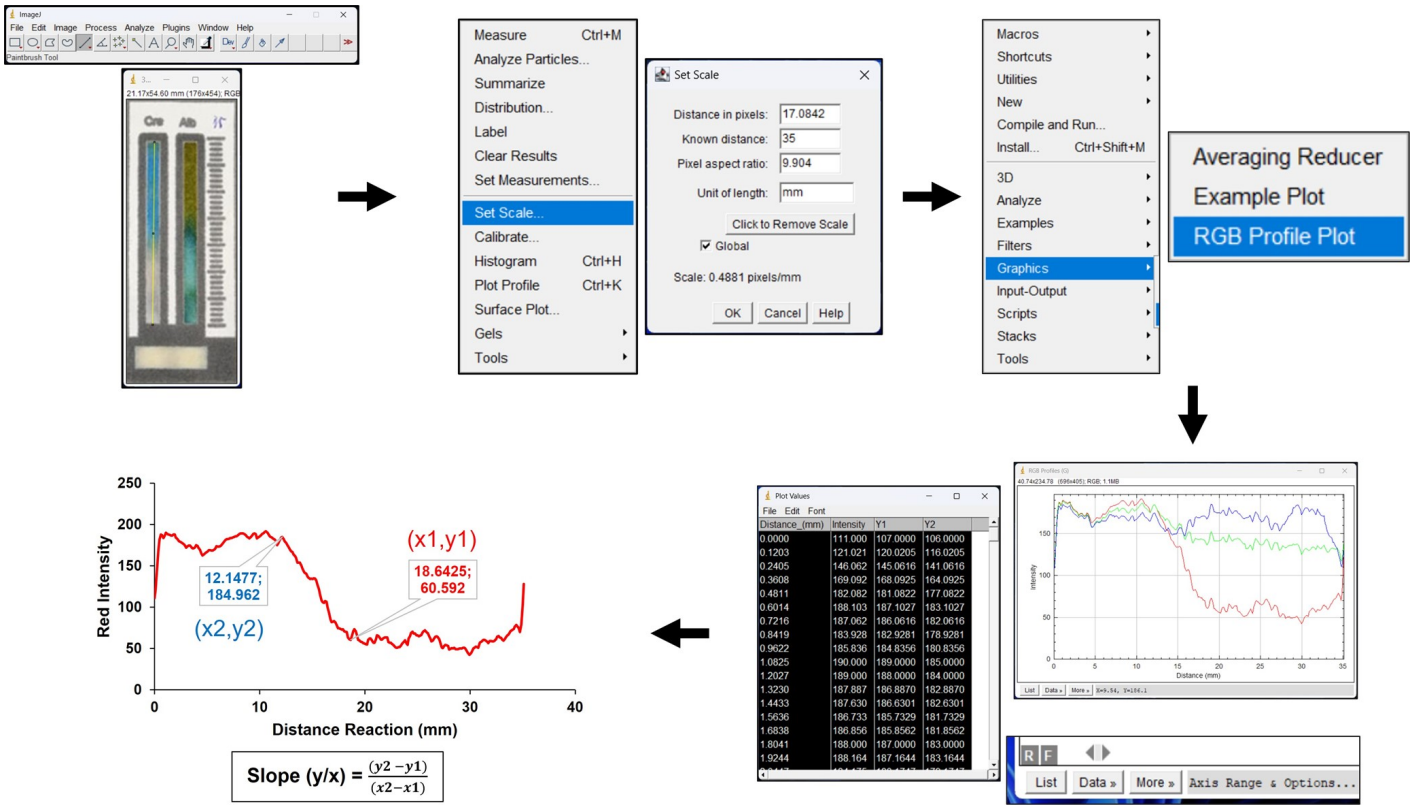

Figure 3. Analysis of The Sharpness of Color Boundaries in The Reaction Distance Using ImageJ

was optimized which includes concentration of CAS and BCG, number of reagent immobilization (CAS-Pd^{2+} and BCG-AuNPs), and reaction time. Linearity was evaluated by analyzing the reaction distance for varying ACR levels: 30, 100, 200, 300, and 400 mg/g. These range ACR levels was selected based on the standard urine levels of healthy patients (<30 mg/g), microalbuminuria (30 – 300 mg/g), and macroalbuminuria (>300 mg/g). It is used to represent the kidney condition of patients based on the ACR levels in urine samples (Persson and Rossing, 2018; Vaidya and Aeddula, 2024). Precision was determined by six measurements of 100 mg/g ACR solution. Accuracy was evaluated by analyzing a real human urine sample and comparing the results with those obtained using a hospital-standard urine autoanalyzer.

2.1.4 Urinary Albumin-Creatinine Ratio Test

Testing on human urine samples was conducted following ethical clearance with approval number 400/094/K.3/302/2021. A total of 15 urine samples were collected from Dr. Saiful Anwar General Hospital, Malang, Indonesia. Each sample was analyzed using the proposed method, with tests performed in triplicate to enhance the accuracy of the results. The findings were then compared with those obtained from a standard urinalysis device (urine auto analyzer) as reported by Dr. Saiful Anwar General Hospital. The test results were evaluated and categorized into three groups based on the albumin levels detected in the urine: normal, microalbuminuria, and macroalbuminuria.

3. RESULTS AND DISCUSSION

3.1 Principle of Reaction Detection

The principle of reaction detection in this study involves detecting albumin using the colored BCG reagent modified with AuNPs and detecting creatinine through ligand exchange reaction between CAS-Pd^{2+} and creatinine.

The Bromocresol Green (BCG) reagent was modified with gold nanoparticles (AuNPs) to enhance the sensitivity and selectivity of the analysis (Bolaños et al., 2019). AuNPs interact with the albumin reagent to form aggregations, which result in a more pronounced color change, thereby improving detection sensitivity (Wang et al., 2019). The interaction of albumin with the BCG reagent is illustrated in Figure 4 (left). The mechanism of this reaction begins with the mixing of BCG and AuNPs, where BCG serves as a colorimetric reagent that binds to albumin through electrostatic interactions between the phenyl groups of BCG and the carbonyl groups on albumin. When albumin is introduced into the BCG-AuNPs solution, it binds to BCG, causing a conformational change in the BCG molecules and promoting further interactions with AuNPs. The gold nanoparticles, known for their localized surface plasmon resonance (LSPR) properties, enhance the optical response by increasing the intensity of the color change.

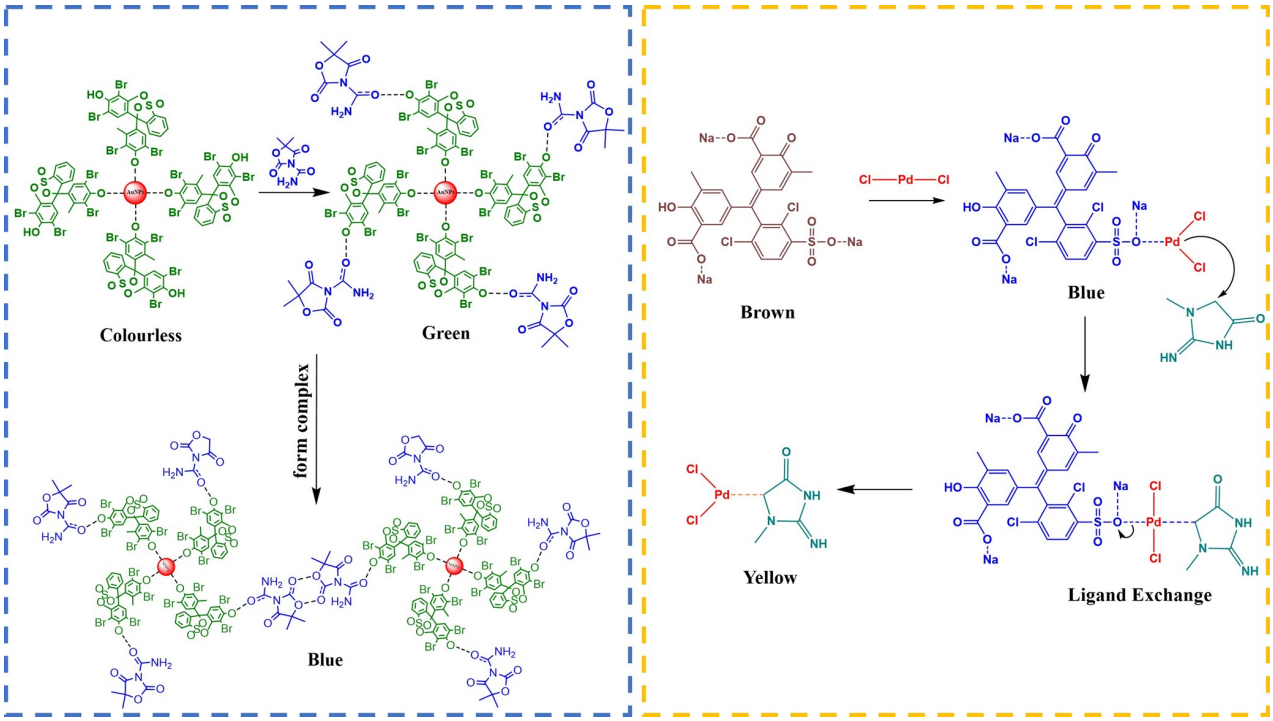

Figure 4. Interaction of Albumin with BCG (Left) and Reaction of Creatinine with CAS-Pd^{2+} (Right)

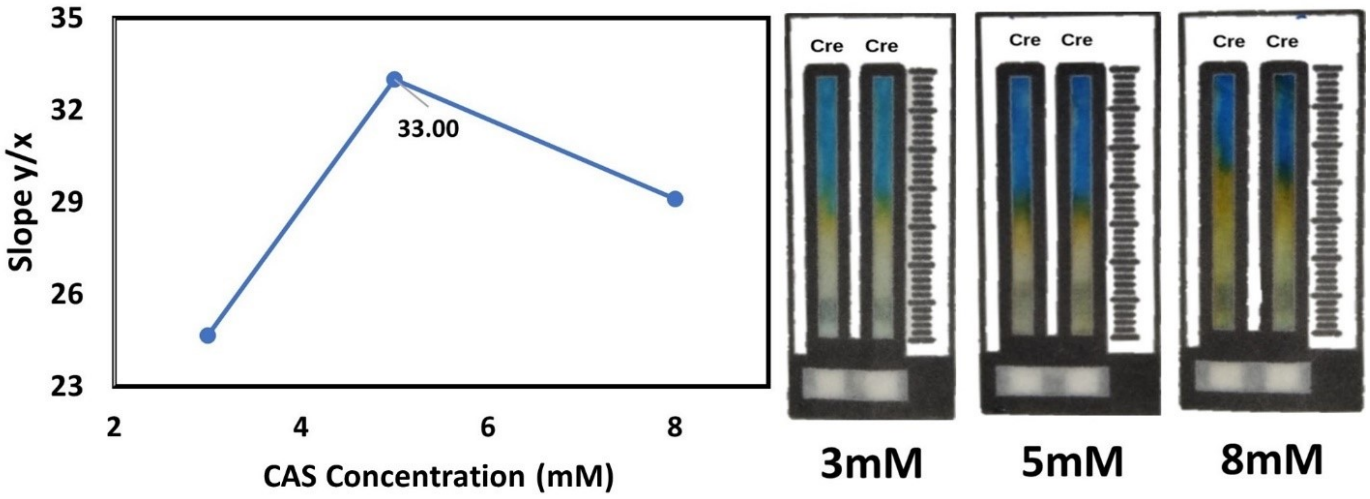

Figure 5. Effect of CAS-Pd^{2+} Reagent Concentration on Color Change and Slope Intensity for Creatinine Detection

This interaction leads to the formation of larger nanoparticle aggregates, altering the surface plasmon distribution and producing a more significant color shift in the solution. This shift results in a more intense color change compared to the reaction of BCG with albumin alone, allowing for the detection of lower concentrations of albumin with enhanced sensitivity.

The reaction mechanism involving Chrome Azurol S (CAS) and Palladium Chloride ($PdCl_2$) for creatinine detection via a modified Jaffe approach comprises a series of carefully designed chemical interactions aimed at enhancing the selectivity and sensitivity of detection. The process begins with the formation of a CAS-Pd^{2+} complex when CAS reacts with Pd^{2+} ions from $PdCl_2$ through a ligand exchange reaction. This CAS-Pd^{2+} complex exhibits distinct optical and chemical properties compared to unmodified CAS, making it more selective for creatinine detection. When the CAS-Pd^{2+} complex is introduced into a sample containing creatinine, creatinine acts as a ligand capable of binding with Pd^{2+} ions within the complex.

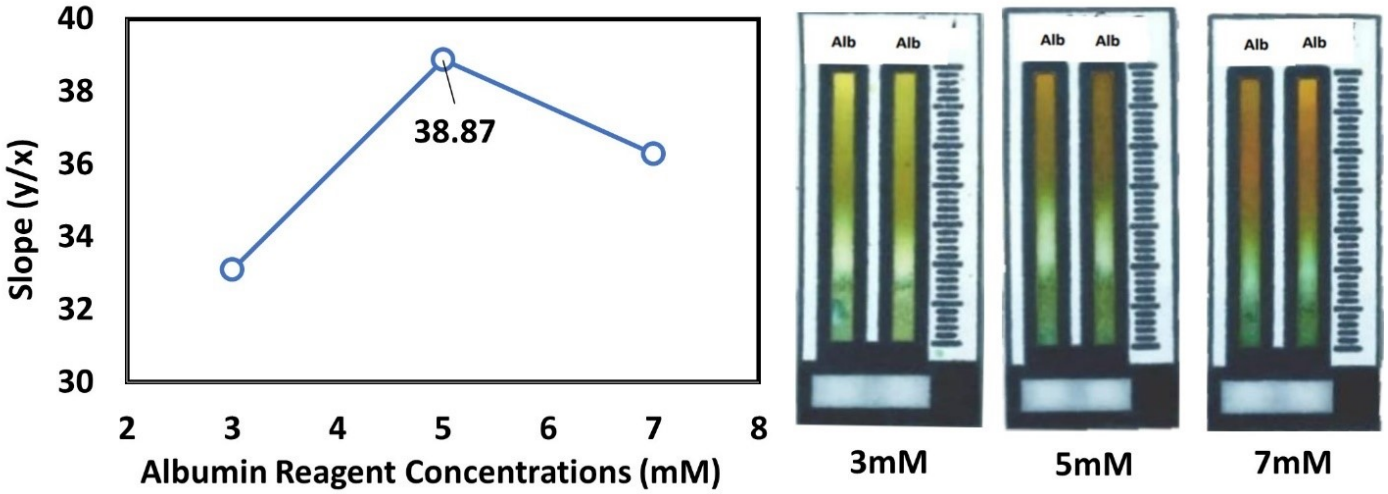

Figure 6. Effect of BCG-AuNPs Reagent Concentration on Color Change and Slope Intensity for Albumin Detection

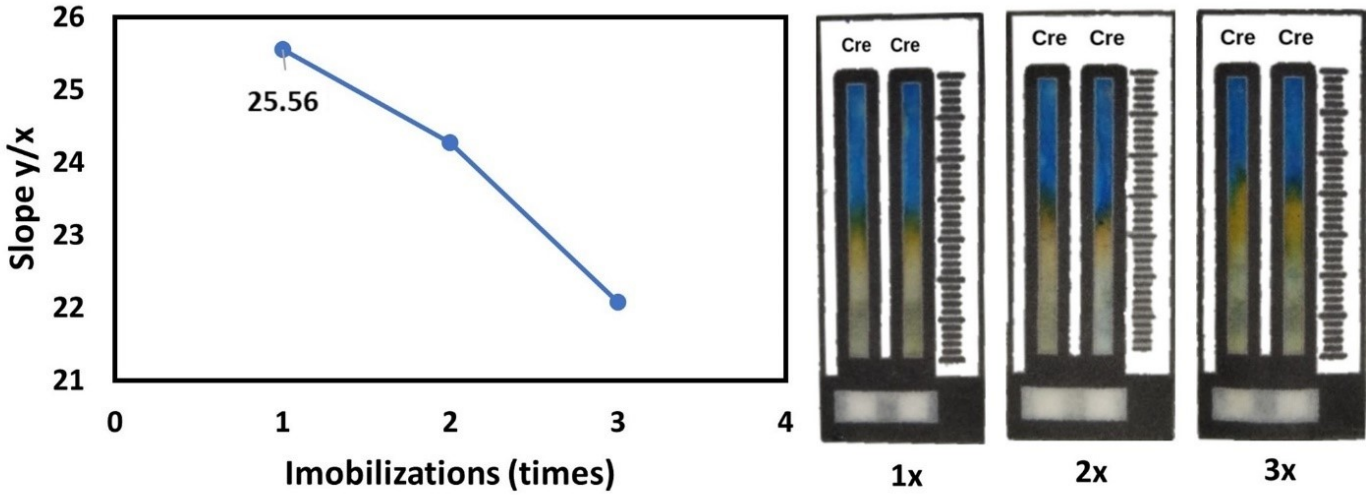

Figure 7. Effect of CAS-Pd^{2+} Reagent Immobilization on Color Change and Slope Intensity for Creatinine Detection

Through a ligand exchange reaction, creatinine displaces CAS as the primary ligand, forming a new complex, Cre-Pd^{2+} (Snee et al., 2005). The ligand exchange reaction between CAS-Pd^{2+} and creatinine is illustrated in Figure 4 (right).

The formation of the Cre-Pd^{2+} complex is accompanied by a significant shift in the light absorption spectrum, resulting in a color change that can be observed visually or quantified using spectrophotometric analysis. This color change provides a direct indication of the presence of creatinine in the sample and allows for more accurate determination of creatinine concentration. The incorporation of Pd^{2+} into the CAS-Pd^{2+} complex reduces interference from other compounds that often compromise measurements in the traditional Jaffe method, which involves creatinine reacting with picric acid under alkaline conditions and can lead to nonspecific signals.

Therefore, the modification of CAS with $PdCl_2$ to form the CAS-Pd^{2+} complex enhances the selectivity and accuracy of creatinine detection. This reaction is less susceptible to external interference, yielding more reliable results in biological sample analysis. This comprehensive mechanism allows for highly specific creatinine detection through a clear colorimetric response, positioning this method as an advanced alternative to the conventional Jaffe reaction approach.

3.1.1 Effect of Reagent Concentration on Slope Intensity

The concentration of reagents used in this study significantly affects the color change and the slope value measured by ImageJ software. ImageJ analysis is employed to determine the slope value (y/x), where x represents the reaction distance and y denotes the color intensity. The slope value, which indicates

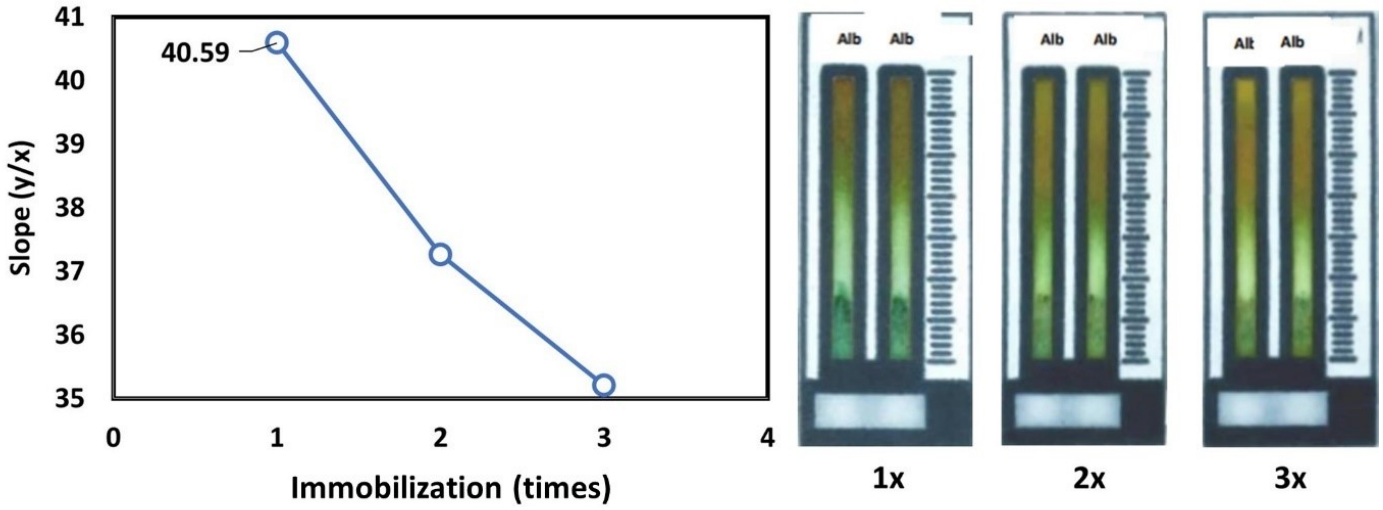

Figure 8. Effect of BCG-AuNPs Reagent Immobilization on Color Change and Slope Intensity for Albumin Detection

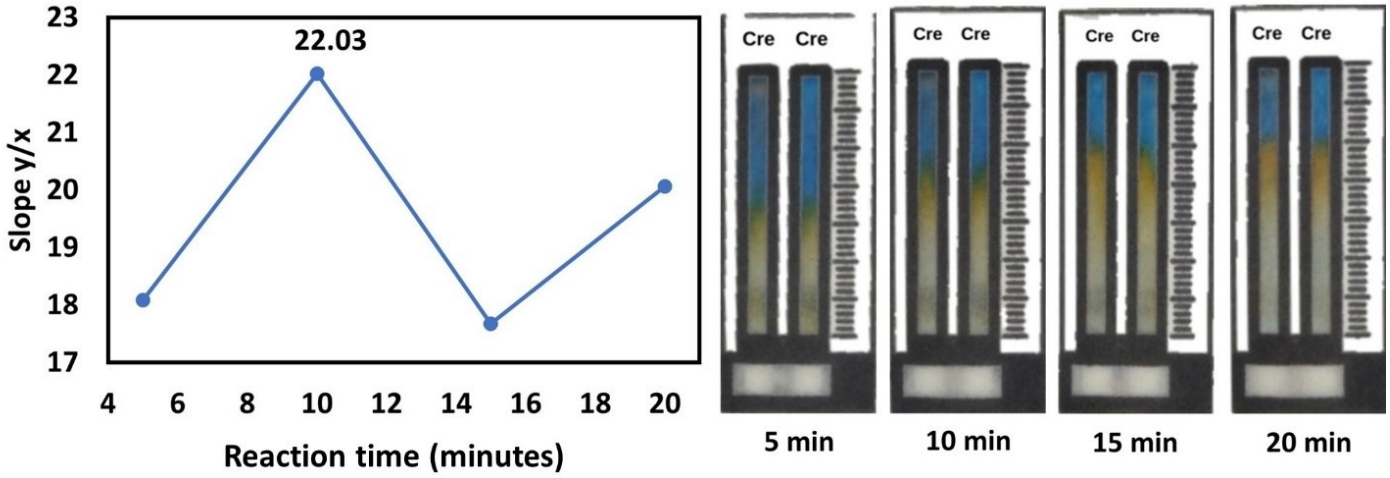

Figure 9. . Effect of Reaction Time on Color Change and Slope Intensity for Creatinine Detection Using CAS-Pd^{2+} Reagent

the firmness of the color change in the reaction zone, is plotted on a graph for assessment. A higher slope value corresponds to a more pronounced color change, while a lower slope value suggests a more gradual and less discernible color transition. For optimization of reagent concentrations, CAS was tested at 3, 5, and 8 mM, while BCG concentrations were tested at 3, 5, and 7 mM. The test samples used for creatinine detection were a 1000 mg/dL creatinine standard solution, and for albumin detection, a 100 mg/dL albumin standard solution was employed.

The results of the creatinine reagent concentration optimization are shown in Figure 5. Visual investigation revealed that a 3 mM concentration of Chrome Azurol S (CAS) produced a discernible color change, though the intensity was relatively weak. At 5 mM, the color change became more pronounced, with a clearer and more intense hue compared to the 3 mM concentration. The 8 mM CAS concentration demonstrated the most intense color change among all tested concentrations. These visual findings were corroborated by further analysis using ImageJ software. The lowest slope value was recorded at a concentration of 3 mM, while the highest slope value, 33.00, was observed at 5 mM CAS. The slope value for the 8 mM concentration was lower than that for 5 mM, likely due to the extended yellow color caused by residual reactions between CAS-Pd^{2+} and creatinine, which ultimately reduced the slope. Based on both visual observation and ImageJ analysis, the optimal concentration for CAS was identified as 5 mM. At this concentration, CAS forms a ligand with Pd^{2+} efficiently, producing a color change that is distinct and easier to detect compared to other concentrations. This optimal condition was

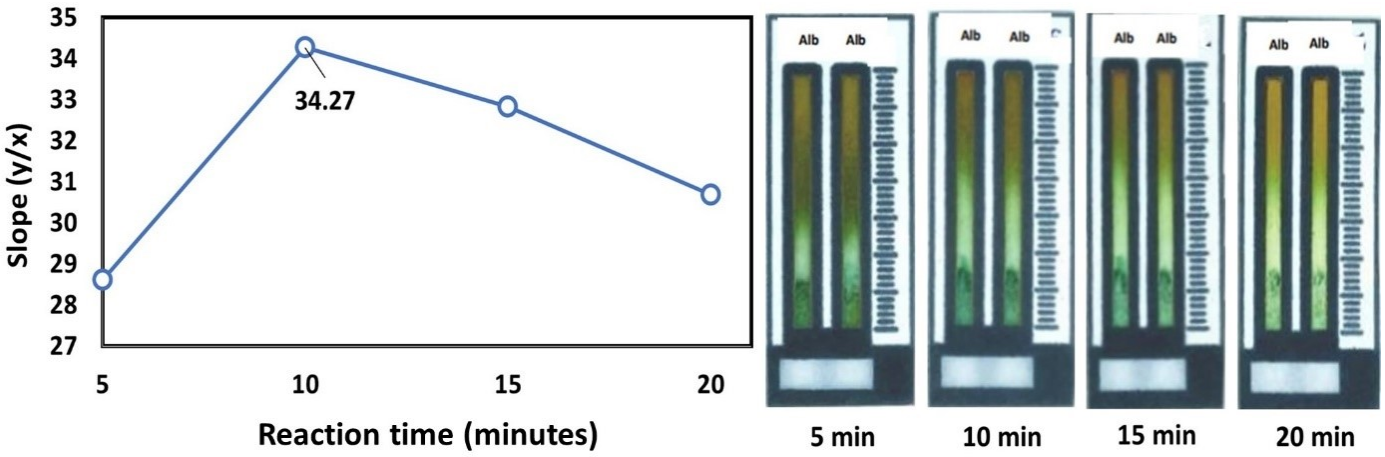

Figure 10. Effect of Reaction Time on Color Change and Slope Intensity for Albumin Detection Using BCG-AuNPs Reagent

applied in subsequent optimization procedures.

The results of the albumin reagent concentration optimization are illustrated in Figure 6. Visual inspection showed that different concentrations of Bromocresol Green (BCG) resulted in varying propagation distances of the reaction. At a concentration of 3 mM, the propagation distance was relatively short, the color change was poorly defined, and the boundary between colors was difficult to observe. In contrast, BCG concentrations of 5 mM and 7 mM exhibited a more distinct color boundary, with the 5 mM concentration demonstrating the greatest propagation distance. The highest slope value, 38.87, was recorded at the 5 mM BCG concentration. This concentration promotes a strong interaction between albumin and gold nanoparticles (AuNPs), leading to the formation of a complete corona protein. This full corona protein interacts effectively with BCG, resulting in a more extensive and pronounced color propagation compared to other concentrations. Furthermore, the formation of the corona protein helps reduce cellulose reactions on the paper, allowing for a clearer and more distinct color change. Based on these findings, the optimal BCG concentration for albumin detection was determined to be 5 mM, as it produced the highest slope value and resulted in a color change from green to a bright greenish-white, which was easily discernible by visual inspection (Bolaños et al., 2019).

3.1.2 Effect of Reagent Immobilization Number on Slope Intensity

Reagent immobilization was performed by pipetting the reagent into the reaction zone in successive steps, ranging from one to three repetitions. This process was designed to assess the impact of repetitive reagent application on the color intensity produced on the 3D-μPADs paper. The concentrations used for this immobilization were based on the optimal conditions determined in the prior optimization phase, specifically, 5 mM for both CAS and BCG reagents. For the test samples, a 1000 mg/dL creatinine standard solution was used for creatinine detection, while a 100 mg/dL albumin standard solution was used for albumin detection.

The results of CAS reagent immobilization optimization are presented in Figure 7. For one-time immobilization, the gradient of the color change was quite distinct and could be observed clearly with the naked eye. However, with two-time and three-time immobilizations, a prolonged residual reaction was observed, leaving a yellow hue beneath the blue color change. This indicates the presence of residual reactions between CAS-Pd^{2+} and creatinine. The lowest slope value was recorded for three-time immobilization, while the highest slope value, 25.56, was achieved with one-time immobilization. Although the color change was visible in all cases, increased repetitions led to the appearance of residual reactions beneath the observed color changes. As a result, the slope values obtained using ImageJ software were lower for two- and three-time immobilizations compared to the one-time immobilization.

The detection results for the BCG reagent immobilization optimization are presented in Figure 7. Visual observation showed that one-time immobilization of the reagent produced the best propagation distance and the most distinct color change. In contrast, with two-time and three-time immobilizations, the color changes were less pronounced and more diffused, making them harder to observe by eye. The highest slope value, 40.59, was achieved with one-time immobilization. The slope values for the two- and three-time immobilizations were lower because the reagents did not distribute evenly across the entire surface of the sample zone, leading to suboptimal reactions. In one-time immobilization, the reagents were uniformly spread across the 3D-μPADs surface, allowing the reagent solution to reach reaction equilibrium. This resulted in a clearer, more consistent color change after the addition of the sample solution.

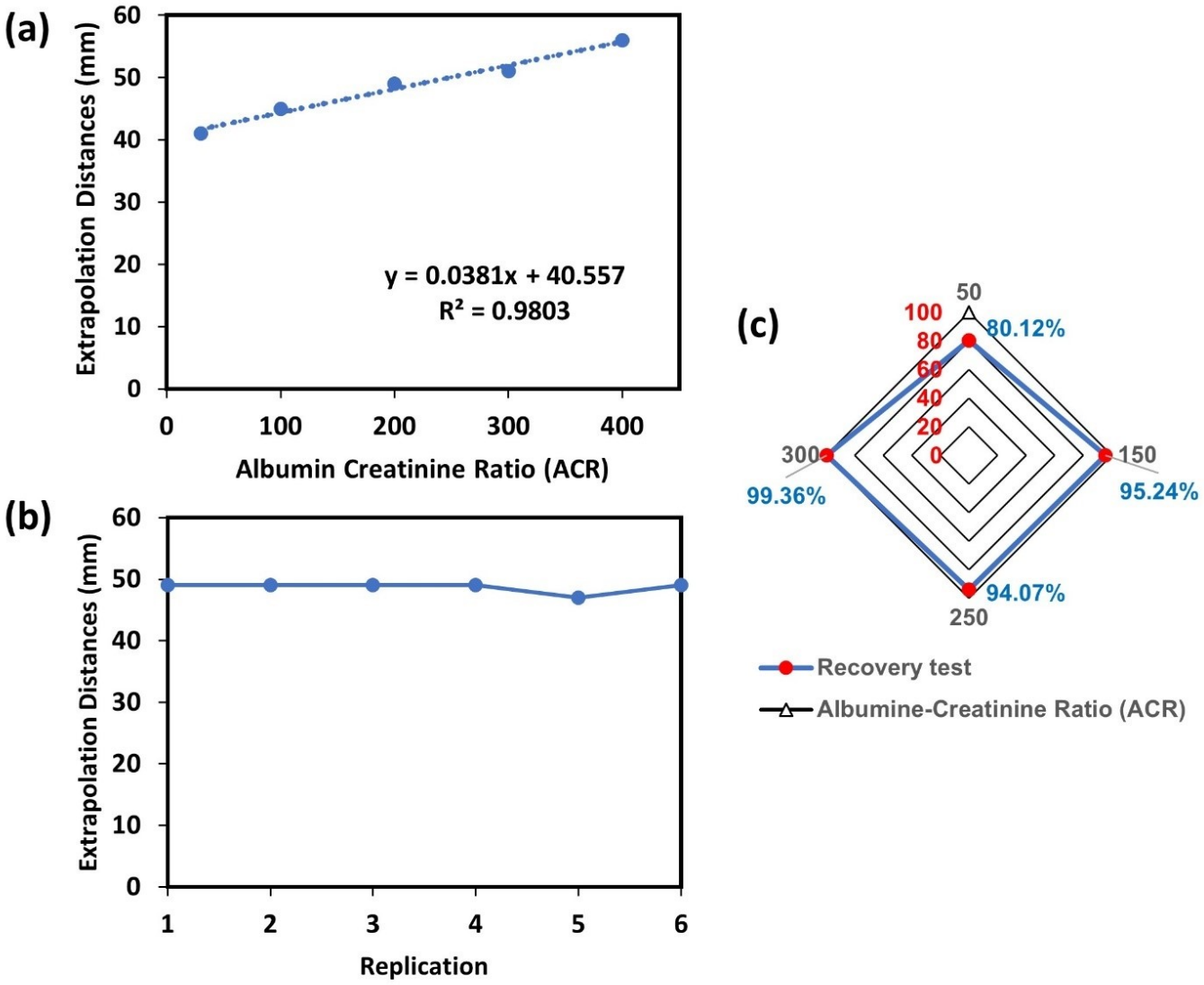

Figure 11. Linearity (a); Precision (b); Recovery test (c) for ACR Detection

3.1.3 Effect of Reaction Time on Slope Intensity

The reaction time optimization was performed by observing the color change in the reaction zone at intervals of 5, 10, 15, and 20 minutes. The aim of this optimization was to determine the optimal reaction time for the interaction between the reagents and the test samples. The reagents used in this study included 5 mM CAS reagent and 5 mM BCG reagent, with each reagent immobilized one time. The test samples consisted of a 1000 mg/dL creatinine standard solution and a 100 mg/dL albumin standard solution. Through this process, the optimal reaction time was identified, allowing for more accurate detection of albumin and creatinine levels.

The results of the CAS reagent reaction time optimization are presented in Figure 9. At the 5-minute observation, the gradient changes had begun to form, but the intensity was not yet fully developed. By 10 minutes, the gradient changes were more distinct and concentrated, resulting in a clear and observable color shift. However, at 15 and 20 minutes, the yellow color gradient became excessively prolonged, making it more challenging to observe the color transition through direct observation. The highest slope value during reaction time optimization was recorded at 10 minutes, with a value of 22.03. The 5-minute reaction time produced the lowest slope because the reaction was not fully optimized, leading to a less intense color change. The 15-minute reaction time yielded a lower slope value due to the overly extended yellow color gradient, which diluted the intensity of the observable reaction distance. Therefore, based on the analysis, 10 minutes was determined to be the optimal reaction time for creatinine detection, producing the most concentrated and clear gradient.

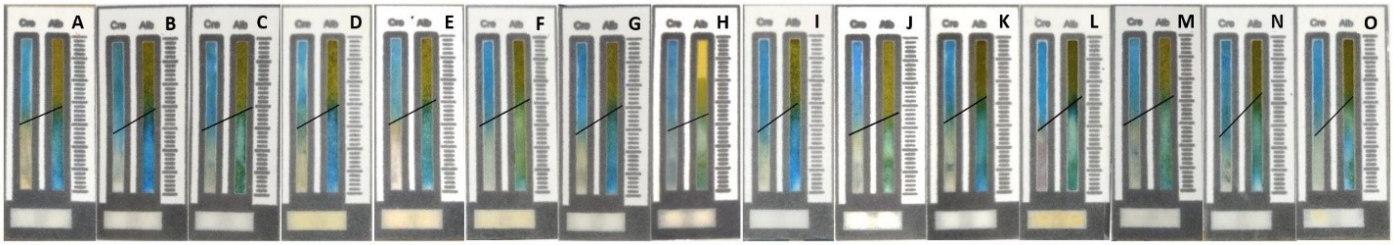

Figure 12. Urinary Albumin-Creatinine Ratio (UACR) Test

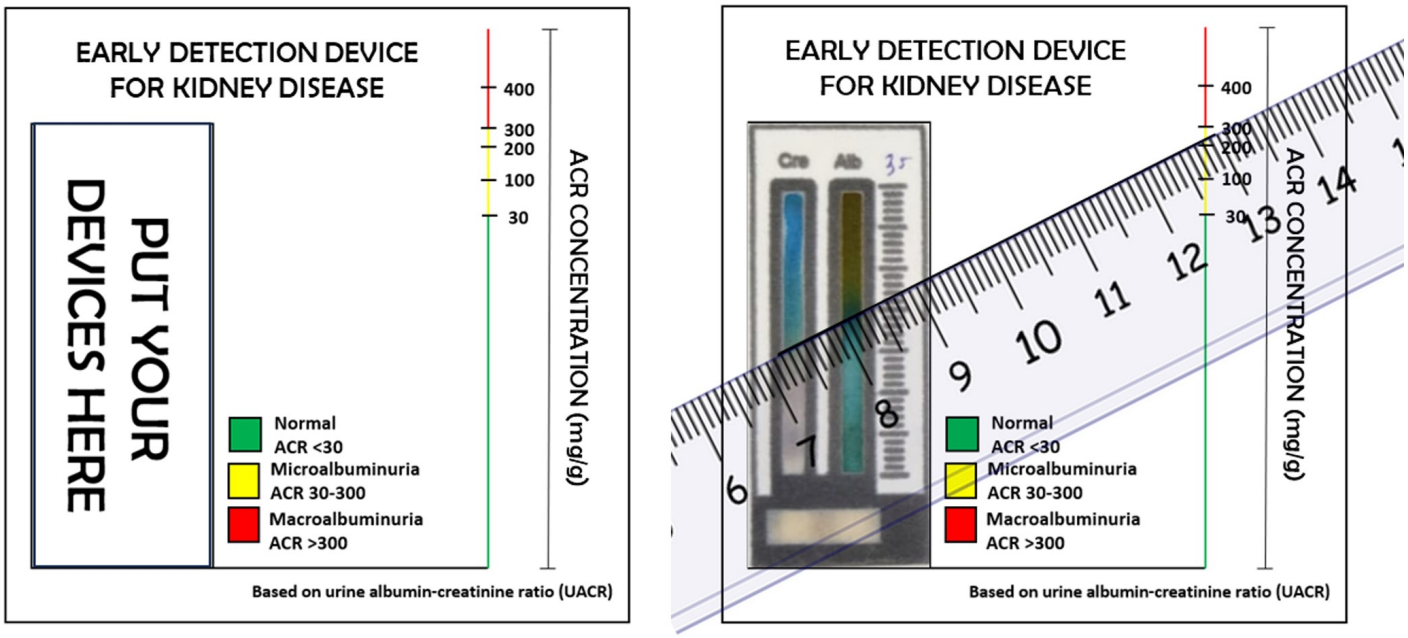

Figure 13. Card Reader for Semiquantitative Analysis of Albumin-Creatinine Ratio

The results of the BCG reagent reaction time optimization are presented in Figure 10. Visual observations indicated that the color changes were uniformly distributed across all reaction times. However, with increasing reaction time, the color propagation became more diffuse. Among the different reaction times, 10 minutes demonstrated the most pronounced and stable color change. The highest slope value, 34.27, was achieved at 10 minutes. This indicates that the optimal reaction conditions for albumin occur within this timeframe, resulting in the formation of a well-defined full corona protein. The extended reaction time reduces interactions between albumin and the paper, leading to more distinct color propagation boundaries. Consequently, a reaction time of 10 minutes is determined to be optimal, as it provides the highest slope value and a clear, stable color change.

3.1.4 Validation Method

The method validation of the developed 3D-μPADs for albumin -creatinine ratio (ACR) analysis was performed under optimized conditions, which were rigorously established through parameter optimization studies. Optimal parameters included a CAS reagent concentration of 5 mM, BCG reagent concentration of 5 mM, single-layer immobilization of each reagent, and a reaction time of 10 minutes. These conditions facilitated rapid and stable colorimetric reactions essential for consistent detection. The reagent volumes applied were 6 μL for CAS, 8 μL for BCG, and a sample volume of 35 μL, with BCG pH adjusted to 4. Furthermore, a 1:5 volume ratio of gold nanoparticles (AuNPs) to Bromocresol Green (BCG) was used, optimizing the dye-binding response.

For linearity test, artificial urine samples were spiked to create albumin index solutions covering a clinically relevant ACR range (30 to 400 mg/g, x-axis), as depicted in Figure 11, which demonstrates the linear response across this range. The

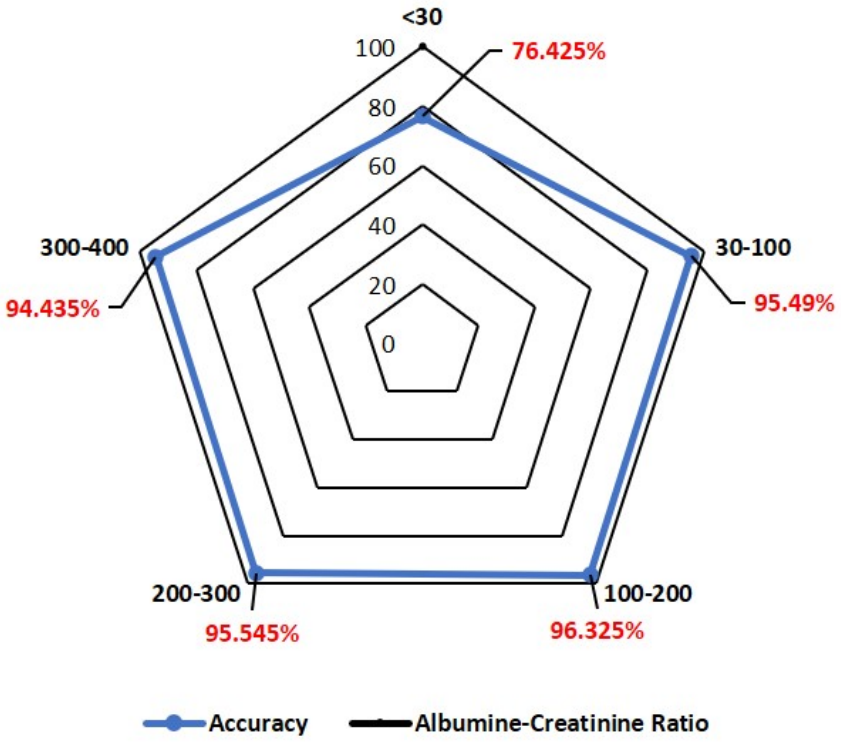

Figure 14. Accuracy Results Graph of UACR

extrapolation distances (y-axis) where obtained by assessing the gradient created by the differing reaction lengths between the albumin and creatinine detection zones. This extrapolated distance, which spans the two endpoints of the reaction, is then input into a linear regression equation developed from calibration data to convert the measured distance into the ACR level of the sample.

A linear regression analysis was performed to correlate color-change distance with ACR levels, yielding a high R^2 value (0.9803), indicative of a strong linear relationship. This defined linear range confirms the 3D-μPADs capability for accurate ACR detection in urine samples. The linear regression provided a quantitative approach to the accuracy of the proposed method, establishing reaction thresholds based on visually detectable color shifts at each detection channel of 3D-μPADs, which reflect albumin and creatinine interactions with the appropriate reagents. Specifically, albumin triggered a color transition in BCG-AuNPs from yellow to blue via dye-binding, while the CAS-Pd^{2+}-creatinine interaction resulted in color shifts from brownish to blue, and then to yellow, as creatinine formed the Cre-Pd^{2+} complex (Hiraoka et al., 2020). The sensitivity of the measurements was also evaluated in this study, which resulted in the limit of detection (LOD) of about 11 mg/g ACR, indicating wide range ACR detection from normal to macroalbuminuria.

The precision was evaluated by repeating the analysis six times at an ACR level of 100 mg/g. The relative standard deviation (%RSD) was 1.53%, confirming high reproducibility of the 3D-μPADs devices. Recovery test was determined by comparing the measured reaction distance with known standard ACR levels, ranging from 50 to 350 mg/g at 50 mg/g intervals. Recovery test was calculated based on the difference between expected and observed values, yielding recoveries from 80.12% to 99.36%. This high recovery indicates that the 3D-μPADs not only produces values close to true ACR levels but also effectively provides reliable and accurate ACR results, which is useful for early detection of nephropathy.

3.1.5 Real Human Urine Sample Detection

Albuminuria is a condition characterized by elevated levels of albumin in the urine, signaling potential kidney dysfunction. Under normal circumstances, albumin remains within the bloodstream. However, its presence in urine indicates that the kidneys may be damaged or impaired. Albuminuria can be assessed by measuring the urine albumin-to-creatinine ratio (UACR). Chronic Kidney Disease (CKD) classification based on albuminuria is categorized into three levels: normal (UACR <30), microalbuminuria (UACR 30-300), and macroalbuminuria (UACR >300) (Decreased, 2013).

Subsequently, 15 of human urine samples were collected from Dr. Saiful Anwar General Hospital in Malang City and tested on 3D-μPADs under the optimized conditions established in previous experiments. Figure 12 illustrates the color change and reaction distances for the urine samples. The ob-

Table 2. Urinary Albumin-Creatinine Ratio (UACR) Analytical Results

Sample Code	UARC Level (mg/g)			%Error	%Accuracy
	Autoalyzer (from Hospital)	3D-μPADs Method			
		Semiquantitative	Quantitative		
A	9.6	<30	11.6 ± 0.47	21.12	78.88
B	14.6	<30	11.6 ± 0	26.03	73.97
C	69.9	30-100	67.1 ± 0.47	3.99	96.01
D	86.1	30-100	90.37 ± 0.82	4.96	95.04
E	94.7	30-100	90.37 ± 0.47	4.58	95.42
F	121.3	100-200	116.61 ± 0	3.86	96.14
G	140	100-200	142.86 ± 1.25	2.04	97.96
H	180	100-200	172.1 ± 0.94	4.39	95.61
I	187.1	100-200	195.35 ± 0.47	4.41	95.59
J	208.4	200-300	224.59 ± 1.25	7.77	92.23
K	214.7	200-300	221.6 ± 0	3.21	96.79
L	235.3	200-300	221.6 ± 0	5.82	94.18
M	250.4	200-300	247.85 ± 0.82	1.02	98.98
N	322.6	300-400	300.34 ± 0.47	6.90	93.10
O	363.7	300-400	379.08 ± 0.94	4.23	95.77
Average				6.96	93.04

served distances in the creatinine and albumin reaction zones were used to determine the intercept distance, which indicates the concentration of ACR in the urine.

In the experimental protocol of semi-quantitative method, 3D-μPADs for ACR measurement were positioned on a card reader, as illustrated in Figure 13. The reaction distances within the albumin and creatinine zones were measured using linear markings with a ruler or stick, corresponding to ACR levels indicated by green, yellow, and red colors on the card reader. This alignment enabled direct interpretation of ACR levels using a colorimetric distance scale, allowing for simplified ACR categorization without the need for sophisticated instrumentation.

An intersection with the green zone (ACR <30 mg/g) indicated normal albumin-creatinine levels, while the yellow zone (ACR 30-300 mg/g) suggested microalbuminuria, prompting further clinical evaluation to confirm the albumin-creatinine ratio. An intersection with the red zone (ACR >300 mg/g) indicated a critical condition, warranting immediate clinical intervention for nephropathy. This semi-quantitative card reader method provides a straightforward approach for early ACR screening, promoting timely nephropathy detection and potentially lowering disease progression risks in resource-limited settings.

The semi-quantitative testing of urine samples using the 3D-μPAD-based method (Table 2) resulted highly reliable results. All the samples tested showed an accuracy rate of 100%, demonstrating that the semi-quantitative method is exceptionally sensitive in detecting albumin-creatinine ratios. This includes accurate identification of ACR levels in the normal range, as well as in the microalbuminuria and macroalbuminuria categories. The findings confirm that the method is effective for distinguishing between different levels of albumin-creatinine ratios with a high accuracy.

The distance-based quantitative method for albumin-creatin ine ratio (ACR) analysis using 3D-microfluidic paper-based analytical devices (3D-μPADs) was assessed using calibration curve as shown in Figure 11a. The analytical evaluation of human urine samples, as outlined in Table 2, revealed an overall accuracy of 93.04% for the 3D-μPADs-based platform, underscoring its accuracy in quantitative analysis. The measurement accuracy of Albumin-to-Creatinine Ratio (ACR) varies across different concentration ranges (Figure 14). For ACR values below 30 mg/g, accuracy tends to be lower (average: 76.43%) because the original concentration on the sample as reported by the hospital (A-B sample) is near the detection limit of the proposed method. For samples with ACR values between 30-100 mg/g (samples C-E), the average accuracy reaches 95.49%, accompanied by a low standard deviation, indicating consistent and reliable results. Samples with ACR values between 100-200 mg/g (samples F-I) achieve an average accuracy of 96.33%, though with a relatively higher standard deviation, suggesting potential variability that could be minimized through repeated testing for more precise measurements.

An average accuracy of 95.55% is recorded for samples with ACR values between 200-300 mg/g (samples J-M), accompanied by a relatively low standard deviation, reflecting high precision within this range. For macroalbuminuria samples with ACR values between 300-400 mg/g (samples N & O), the average accuracy is 94.44%, with a relatively low standard deviation. These results indicate that 3D-μPADs is an effective tool for ACR detection and holds significant potential for early detection of chronic kidney disease in community settings.

4. CONCLUSIONS

This study successfully developed a 3D-μPADs-based method for the simultaneous detection of albumin and creatinine in urine, providing an accessible, low-cost alternative for assessing kidney function. The optimization of reagent concentrations, immobilization, and reaction time enhanced the sensitivity and accuracy of the device. Validation with real human urine samples yielded an accuracy of 93.04%, demonstrating the 3D-μPADs potential for early detection of nephropathy. The simplicity, affordability, and effectiveness of 3D-μPADs highlight their suitability for use in resource-limited settings, where early diagnosis of CKD is crucial to improving patient outcomes. Future work will focus on integrating semi-quantitative card readers for widespread community use, enhancing the applicability of 3D-µPADs in point-of-care diagnostics.

5. ACKNOWLEDGEMENTS

We would like to thank the Institute of Research and Community Services, Brawijaya University for the financial support through The CoE Initiation Strategic Research Scheme (No: 989.2/UN10.C20/2023). Additionally, AS would like to thank the ministry of finance of the Republic of Indonesia for partial support of this work through RISPRO LPDP 2021 (PRJ-033/LPDP/2021).

REFERENCES

Ajdari, N., C. Vyas, S. L. Bogan, B. A. Lwaleed, and B. G. Cousins (2017). Gold Nanoparticle Interactions in Human Blood: A Model Evaluation. *Nanomedicine: Nanotechnology, Biology and Medicine*, **13**(4); 1531–1542

Al-Jaf, S. H. and K. M. Omer (2022). Enhancing of Detection Resolution via Designing of a Multi-Functional 3D Connector Between Sampling and Detection Zones in Distance-Based Microfluidic Paper-Based Analytical Device: Multi-Channel Design for Multiplex Analysis. *Microchimica Acta*, **189**(12); 482

Ariyanti, M., L. Lillah, E. Nasrul, and H. Husni (2018). Correlation of Urine N-Acetyl-Beta-D-Glucosaminidase Activity with Urine Albumin Creatinine Ratio in Type 2 Diabetes Mellitus. *Indonesian Journal of Clinical Pathology and Medical Laboratory*, **23**(3); 275–280

Bolaños, K., M. J. Kogan, and E. Araya (2019). Capping Gold Nanoparticles with Albumin to Improve Their Biomedical Properties. *International Journal of Nanomedicine*, **14**; 6387–6406

Bruzewicz, D. A., M. Reches, and G. M. Whitesides (2008). Low-Cost Printing of Poly(Dimethylsiloxane) Barriers to Define Microchannels in Paper. *Analytical Chemistry*, **80**(9); 3387–3392

Carrilho, E., A. W. Martinez, and G. M. Whitesides (2009). Understanding Wax Printing: A Simple Micropatterning Process for Paper-Based Microfluidics. *Analytical Chemistry*, **81**(16); 7091–7095

Chaiyo, S., K. Kalcher, A. Apilux, O. Chailapakul, and W. Siangproh (2018). A Novel Paper-Based Colorimetry Device for the Determination of the Albumin to Creatinine Ratio. *The Analyst*, **143**(22); 5453–5460

Chapman, D. P., K. M. Gooding, T. J. McDonald, and A. C. Shore (2019). Stability of Urinary Albumin and Creatinine after 12 Months Storage at -20 °C and -80 °C. *Practical Laboratory Medicine*, **15**; e00120

Chen, Q., M. Lu, B. R. Monks, and M. J. Birnbaum (2016). Insulin Is Required to Maintain Albumin Expression by Inhibiting Forkhead Box O1 Protein. *Journal of Biological Chemistry*, **291**(5); 2371–2378

Chen, S.-J., C.-C. Tseng, K.-H. Huang, Y.-C. Chang, and L.-M. Fu (2022). Microfluidic Sliding Paper-Based Device for Point-of-Care Determination of Albumin-to-Creatine Ratio in Human Urine. *Biosensors*, **12**(7); 496

Cheng, J., J. Huang, Q. Xiang, and H. Dong (2023). Hollow Microneedle Microfluidic Paper-Based Chip for Biomolecules Rapid Sampling and Detection in Interstitial Fluid. *Analytica Chimica Acta*, **1255**; 341101

Dai, J., C. Chen, M. Yin, H. Li, W. Li, Z. Zhang, Q. Wang, Z. Du, X. Xu, and Y. Wang (2023). Interactions between Gold Nanoparticles with Different Morphologies and Human Serum Albumin. *Frontiers in Chemistry*, **11**; 1273388

De Tarso Garcia, P., T. M. Garcia Cardoso, C. D. Garcia, E. Carrilho, and W. K. Tomazelli Coltro (2014). A Handheld Stamping Process to Fabricate Microfluidic Paper-Based Analytical Devices with Chemically Modified Surface for Clinical Assays. *RSC Advances*, **4**(71); 37637–37644

Decreased, G. (2013). Definition and classification of CKD. *Kidney Int*, **3**; 19–62

Fortova, M., E. Klapkova, B. Sopko, and R. Prusa (2018). Estimated Total Albumin in Fresh Urine Samples Based on Correlation Between the Roche Immunoturbidimetric and an In-House HPLC Method. *Clinical Laboratory*, **64**(11+12/2018)

Fraser, S. and T. Blakeman (2016). Chronic Kidney Disease: Identification and Management in Primary Care. *Pragmatic and Observational Research*, **7**; 21–32

Hardiyanti, S. A., N. D. Wijaya, L. Krisdiyanti, S. F. Putri, H. Sulistyarti, A. Mulyasuryani, S. P. Sakti, A. Aulanni'am, and A. Sabarudin (2024). Detection of albumin using gold nanoparticles-mediated microfluidic paper-based analytical devices. In *AIP Conference Proceedings*, volume 3068. AIP Publishing

Harish, V., D. Tewari, M. Gaur, A. B. Yadav, S. Swaroop, M. Bechelany, and A. Barhoum (2022). Review on Nanoparticles and Nanostructured Materials: Bioimaging, Biosensing, Drug Delivery, Tissue Engineering, Antimicrobial, and Agro-Food Applications. *Nanomaterials*, **12**(3); 457

Hiraoka, R., K. Kuwahara, Y.-C. Wen, T.-H. Yen, Y. Hiruta, C.-M. Cheng, and D. Citterio (2020). Paper-Based Device for Naked Eye Urinary Albumin/Creatinine Ratio Evaluation. *ACS Sensors*, **5**(4); 1110–1118

Khachornsakkul, K., R. Del-Rio-Ruiz, H. Creasey, G. Widmer, and S. R. Sonkusale (2023). Gold Nanomaterial-Based Mi-

crofluidic Paper Analytical Device for Simultaneous Quantification of Gram-Negative Bacteria and Nitrite Ions in Water Samples. *ACS Sensors*, **8**(11); 4364–4373

Kiconco, R., S. P. Rugera, and G. N. Kiwanuka (2019). Microalbuminuria and Traditional Serum Biomarkers of Nephropathy among Diabetic Patients at Mbarara Regional Referral Hospital in South Western Uganda. *Journal of Diabetes Research*, **2019**; 1–7

Kovesdy, C. P. (2022). Epidemiology of Chronic Kidney Disease: An Update 2022. *Kidney International Supplements*, **12**(1); 7–11

Kusuma, S. A. F., J. A. Harmonis, R. Pratiwi, and A. N. Hasanah (2023). Gold Nanoparticle-Based Colorimetric Sensors: Properties and Application in Detection of Heavy Metals and Biological Molecules. *Sensors*, **23**(19); 8172

Mohamed, A. A.-R., S. I. Khater, A. Hamed Arisha, M. M. M. Metwally, G. Mostafa-Hedeab, and E. S. El-Shetry (2021). Chitosan-Stabilized Selenium Nanoparticles Alleviate Cardio-Hepatic Damage in Type 2 Diabetes Mellitus Model via Regulation of Caspase, Bax/Bcl-2, and Fas/FasL-Pathway. *Gene*, **768**; 145288

Morbioli, G. G., T. Mazzu-Nascimento, A. M. Stockton, and E. Carrilho (2017). Technical Aspects and Challenges of Colorimetric Detection with Microfluidic Paper-Based Analytical Devices (μPADs)—A Review. *Analytica Chimica Acta*, **970**; 1–22

Mousavi, B., F. Tafvizi, and S. Zaker Bostanabad (2018). Green Synthesis of Silver Nanoparticles Using Artemisia Turcomanica Leaf Extract and the Study of Anti-Cancer Effect and Apoptosis Induction on Gastric Cancer Cell Line (AGS). *Artificial Cells, Nanomedicine, and Biotechnology*, **46**(sup1); 499–510

Ng, J. S. and M. Hashimoto (2020). Fabrication of Paper Microfluidic Devices Using a Toner Laser Printer. *RSC Advances*, **10**(50); 29797–29807

Paramasivam, G., N. Kayambu, A. M. Rabel, A. K. Sundramoorthy, and A. Sundaramurthy (2017). Anisotropic Noble Metal Nanoparticles: Synthesis, Surface Functionalization and Applications in Biosensing, Bioimaging, Drug Delivery and Theranostics. *Acta Biomaterialia*, **49**; 45–65

Park, J., R. Shrestha, C. Qiu, A. Kondo, S. Huang, M. Werth, M. Li, J. Barasch, and K. Suszták (2018). Single-Cell Transcriptomics of the Mouse Kidney Reveals Potential Cellular Targets of Kidney Disease. *Science*, **360**(6390); 758–763

Persson, F. and P. Rossing (2018). Diagnosis of Diabetic Kidney Disease: State of the Art and Future Perspective. *Kidney International Supplements*, **8**(1); 2–7

Petersson, S. D. and E. Philippou (2016). Mediterranean Diet, Cognitive Function, and Dementia: A Systematic Review of the Evidence. *Advances in Nutrition*, **7**(5); 889–904

Randviir, E. P. and C. E. Banks (2013). Analytical Methods for Quantifying Creatinine Within Biological Media. *Sensors and Actuators B: Chemical*, **183**; 239–252

Sabarudin, A. (2018). Sequential Injection at Valve Mixing (SI-VM) for Determination of Albumin-Creatinine Ratio in Urine. *Oriental Journal of Chemistry*, **34**(2); 730–734

Sarigul, N., F. Korkmaz, and Kurultak (2019). A New Artificial Urine Protocol to Better Imitate Human Urine. *Scientific Reports*, **9**(1); 20159

Snee, P. T., J. Shanoski, and C. B. Harris (2005). Mechanism of Ligand Exchange Studied Using Transition Path Sampling. *Journal of the American Chemical Society*, **127**(4); 1286–1290

Songjaroen, T., W. Dungchai, O. Chailapakul, and W. Laiwattanapaisal (2011). Novel, Simple and Low-Cost Alternative Method for Fabrication of Paper-Based Microfluidics by Wax Dipping. *Talanta*, **85**(5); 2587–2593

Srivastava, A., S. K. Chopra, and P. R. Dasgupta (2009). Biochemical Analysis of Human Seminal Plasma II. Protein, Non-Protein Nitrogen, Urea, Uric Acid and Creatine*. *Andrologia*, **16**(3); 265–268

Sulehri, M. A. and N. M. Sheikh (2009). Chronic Renal Failure: Association of Diabetes Mellitus. *The Professional Medical Journal*, **16**(4); 532–536

Sununta, S., P. Rattanarat, O. Chailapakul, and N. Praphairaksit (2018). Microfluidic Paper-Based Analytical Devices for Determination of Creatinine in Urine Samples. *Analytical Sciences*, **34**(1); 109–113

Thompson, L. E. and M. S. Joy (2022). Endogenous markers of kidney function and renal drug clearance processes of filtration, secretion, and reabsorption. *Current Opinion in Toxicology*, **31**; 100344

Tkáčiková, S., I. Talian, and J. Sabo (2020). Optimization of Urine Sample Preparation for Shotgun Proteomics. *Open Chemistry*, **18**(1); 850–856

Trinh, K. T. L., W. R. Chae, and N. Y. Lee (2022). Recent Advances in the Fabrication Strategies of Paper-Based Microfluidic Devices for Rapid Detection of Bacteria and Viruses. *Microchemical Journal*, **180**; 107548

Vaidya, S. R. and N. R. Aeddula (2024). Chronic kidney disease. In *StatPearls [Internet]*. StatPearls Publishing

Wang, G., C. Yan, S. Gao, and Y. Liu (2019). Surface Chemistry of Gold Nanoparticles Determines Interactions with Bovine Serum Albumin. *Materials Science and Engineering: C*, **103**; 109856

Wang, S., L. Ge, X. Song, J. Yu, S. Ge, J. Huang, and F. Zeng (2012). Paper-Based Chemiluminescence ELISA: Lab-on-Paper Based on Chitosan Modified Paper Device and Wax-Screen-Printing. *Biosensors and Bioelectronics*, **31**(1); 212–218

Yamada, K., T. G. Henares, K. Suzuki, and D. Citterio (2015). Paper-Based Inkjet-Printed Microfluidic Analytical Devices. *Angewandte Chemie International Edition*, **54**(18); 5294–5310

Yang, F., L. Zhang, H. Wu, H. Zou, and Y. Du (2014). Clinical Analysis of Cause, Treatment and Prognosis in Acute Kidney Injury Patients. *PLoS ONE*, **9**(2); e85214

Yang, J., X. Wang, Y. Sun, B. Chen, F. Hu, C. Guo, and T. Yang (2022). Recent Advances in Colorimetric Sensors Based on Gold Nanoparticles for Pathogen Detection. *Biosensors*, **13**(1); 29

Yumang, A. N., P. B. Cruz, and C. J. G. Valenzuela (2021). Liquid Chromatography Microfluidics for Detection and Quantification of Urine Albumin Using Linear Regression Method. In *2021 11th International Conference on Biomedical Engineering and Technology*. pages 158–163

Zhang, X., X. Fan, Y. Wang, F. Lei, L. Li, J. Liu, and P. Wu (2020). Highly Stable Colorimetric Sensing by Assembly of Gold Nanoparticles with SYBR Green I: From Charge Screening to Charge Neutralization. *Analytical Chemistry*, **92**(1); 1455–1462

